SLAC-PUB-13556
June 2009

Search for the Rare Leptonic Decays $B^+ \to \ell^+\nu_\ell$ ($\ell = e, \mu$)

B. Aubert,[1] Y. Karyotakis,[1] J. P. Lees,[1] V. Poireau,[1] E. Prencipe,[1] X. Prudent,[1] V. Tisserand,[1] J. Garra Tico,[2] E. Grauges,[2] M. Martinelli[ab],[3] A. Palano[ab],[3] M. Pappagallo[ab],[3] G. Eigen,[4] B. Stugu,[4] L. Sun,[4] M. Battaglia,[5] D. N. Brown,[5] L. T. Kerth,[5] Yu. G. Kolomensky,[5] G. Lynch,[5] I. L. Osipenkov,[5] K. Tackmann,[5] T. Tanabe,[5] C. M. Hawkes,[6] N. Soni,[6] A. T. Watson,[6] H. Koch,[7] T. Schroeder,[7] D. J. Asgeirsson,[8] B. G. Fulsom,[8] C. Hearty,[8] T. S. Mattison,[8] J. A. McKenna,[8] M. Barrett,[9] A. Khan,[9] A. Randle-Conde,[9] V. E. Blinov,[10] A. D. Bukin,[10,*] A. R. Buzykaev,[10] V. P. Druzhinin,[10] V. B. Golubev,[10] A. P. Onuchin,[10] S. I. Serednyakov,[10] Yu. I. Skovpen,[10] E. P. Solodov,[10] K. Yu. Todyshev,[10] M. Bondioli,[11] S. Curry,[11] I. Eschrich,[11] D. Kirkby,[11] A. J. Lankford,[11] P. Lund,[11] M. Mandelkern,[11] E. C. Martin,[11] D. P. Stoker,[11] S. Abachi,[12] C. Buchanan,[12] H. Atmacan,[13] J. W. Gary,[13] F. Liu,[13] O. Long,[13] G. M. Vitug,[13] Z. Yasin,[13] L. Zhang,[13] V. Sharma,[14] C. Campagnari,[15] T. M. Hong,[15] D. Kovalskyi,[15] M. A. Mazur,[15] J. D. Richman,[15] T. W. Beck,[16] A. M. Eisner,[16] C. A. Heusch,[16] J. Kroseberg,[16] W. S. Lockman,[16] A. J. Martinez,[16] T. Schalk,[16] B. A. Schumm,[16] A. Seiden,[16] L. Wang,[16] L. O. Winstrom,[16] C. H. Cheng,[17] D. A. Doll,[17] B. Echenard,[17] F. Fang,[17] D. G. Hitlin,[17] I. Narsky,[17] T. Piatenko,[17] F. C. Porter,[17] R. Andreassen,[18] G. Mancinelli,[18] B. T. Meadows,[18] K. Mishra,[18] M. D. Sokoloff,[18] P. C. Bloom,[19] W. T. Ford,[19] A. Gaz,[19] J. F. Hirschauer,[19] M. Nagel,[19] U. Nauenberg,[19] J. G. Smith,[19] S. R. Wagner,[19] R. Ayad,[20,†] A. Soffer,[20,‡] W. H. Toki,[20] R. J. Wilson,[20] E. Feltresi,[21] A. Hauke,[21] H. Jasper,[21] T. M. Karbach,[21] J. Merkel,[21] A. Petzold,[21] B. Spaan,[21] K. Wacker,[21] M. J. Kobel,[22] R. Nogowski,[22] K. R. Schubert,[22] R. Schwierz,[22] A. Volk,[22] D. Bernard,[23] G. R. Bonneaud,[23] E. Latour,[23] M. Verderi,[23] P. J. Clark,[24] S. Playfer,[24] J. E. Watson,[24] M. Andreotti[ab],[25] D. Bettoni[a],[25] C. Bozzi[a],[25] R. Calabrese[ab],[25] A. Cecchi[ab],[25] G. Cibinetto[ab],[25] E. Fioravanti[ab],[25] P. Franchini[ab],[25] E. Luppi[ab],[25] M. Munerato[ab],[25] M. Negrini[ab],[25] A. Petrella[ab],[25] L. Piemontese[a],[25] V. Santoro[ab],[25] R. Baldini-Ferroli,[26] A. Calcaterra,[26] R. de Sangro,[26] G. Finocchiaro,[26] S. Pacetti,[26] P. Patteri,[26] I. M. Peruzzi,[26,§] M. Piccolo,[26] M. Rama,[26] A. Zallo,[26] R. Contri[ab],[27] E. Guido,[27] M. Lo Vetere[ab],[27] M. R. Monge[ab],[27] S. Passaggio[a],[27] C. Patrignani[ab],[27] E. Robutti[a],[27] S. Tosi[ab],[27] K. S. Chaisanguanthum,[28] M. Morii,[28] A. Adametz,[29] J. Marks,[29] S. Schenk,[29] U. Uwer,[29] F. U. Bernlochner,[30] V. Klose,[30] H. M. Lacker,[30] D. J. Bard,[31] P. D. Dauncey,[31] M. Tibbetts,[31] P. K. Behera,[32] M. J. Charles,[32] U. Mallik,[32] J. Cochran,[33] H. B. Crawley,[33] L. Dong,[33] V. Eyges,[33] W. T. Meyer,[33] S. Prell,[33] E. I. Rosenberg,[33] A. E. Rubin,[33] Y. Y. Gao,[34] A. V. Gritsan,[34] Z. J. Guo,[34] N. Arnaud,[35] J. Béquilleux,[35] A. D'Orazio,[35] M. Davier,[35] D. Derkach,[35] J. Firmino da Costa,[35] G. Grosdidier,[35] F. Le Diberder,[35] V. Lepeltier,[35] A. M. Lutz,[35] B. Malaescu,[35] S. Pruvot,[35] P. Roudeau,[35] M. H. Schune,[35] J. Serrano,[35] V. Sordini,[35,¶] A. Stocchi,[35] G. Wormser,[35] D. J. Lange,[36] D. M. Wright,[36] I. Bingham,[37] J. P. Burke,[37] C. A. Chavez,[37] J. R. Fry,[37] E. Gabathuler,[37] R. Gamet,[37] D. E. Hutchcroft,[37] D. J. Payne,[37] C. Touramanis,[37] A. J. Bevan,[38] C. K. Clarke,[38] F. Di Lodovico,[38] R. Sacco,[38] M. Sigamani,[38] G. Cowan,[39] S. Paramesvaran,[39] A. C. Wren,[39] D. N. Brown,[40] C. L. Davis,[40] A. G. Denig,[41] M. Fritsch,[41] W. Gradl,[41] A. Hafner,[41] K. E. Alwyn,[42] D. Bailey,[42] R. J. Barlow,[42] G. Jackson,[42] G. D. Lafferty,[42] T. J. West,[42] J. I. Yi,[42] J. Anderson,[43] C. Chen,[43] A. Jawahery,[43] D. A. Roberts,[43] G. Simi,[43] J. M. Tuggle,[43] C. Dallapiccola,[44] E. Salvati,[44] S. Saremi,[44] R. Cowan,[45] D. Dujmic,[45] P. H. Fisher,[45] S. W. Henderson,[45] G. Sciolla,[45] M. Spitznagel,[45] R. K. Yamamoto,[45] M. Zhao,[45] P. M. Patel,[46] S. H. Robertson,[46] M. Schram,[46] A. Lazzaro[ab],[47] V. Lombardo[a],[47] F. Palombo[ab],[47] S. Stracka[ab],[47] J. M. Bauer,[48] L. Cremaldi,[48] R. Godang,[48,**] R. Kroeger,[48] P. Sonnek,[48] D. J. Summers,[48] H. W. Zhao,[48] M. Simard,[49] P. Taras,[49] H. Nicholson,[50] G. De Nardo[ab],[51] L. Lista[a],[51] D. Monorchio[ab],[51] G. Onorato[ab],[51] C. Sciacca[ab],[51] G. Raven,[52] H. L. Snoek,[52] C. P. Jessop,[53] K. J. Knoepfel,[53] J. M. LoSecco,[53] W. F. Wang,[53] L. A. Corwin,[54] K. Honscheid,[54] H. Kagan,[54] R. Kass,[54] J. P. Morris,[54] A. M. Rahimi,[54] J. J. Regensburger,[54] S. J. Sekula,[54] Q. K. Wong,[54] N. L. Blount,[55] J. Brau,[55] R. Frey,[55] O. Igonkina,[55] J. A. Kolb,[55] M. Lu,[55] R. Rahmat,[55] N. B. Sinev,[55] D. Strom,[55] J. Strube,[55] E. Torrence,[55] G. Castelli[ab],[56] N. Gagliardi[ab],[56] M. Margoni[ab],[56] M. Morandin[a],[56] M. Posocco[a],[56] M. Rotondo[a],[56] F. Simonetto[ab],[56] R. Stroili[ab],[56] C. Voci[ab],[56] P. del Amo Sanchez,[57] E. Ben-Haim,[57] H. Briand,[57] J. Chauveau,[57] O. Hamon,[57] Ph. Leruste,[57] G. Marchiori,[57] J. Ocariz,[57] A. Perez,[57] J. Prendki,[57] S. Sitt,[57] L. Gladney,[58] M. Biasini[ab],[59] E. Manoni[ab],[59] C. Angelini[ab],[60] G. Batignani[ab],[60] S. Bettarini[ab],[60] G. Calderini[ab],[60,††] M. Carpinelli[ab],[60,‡‡] A. Cervelli[ab],[60] F. Forti[ab],[60] M. A. Giorgi[ab],[60] A. Lusiani[ac],[60] M. Morganti[ab],[60] N. Neri[ab],[60] E. Paoloni[ab],[60] G. Rizzo[ab],[60] J. J. Walsh[a],[60]

Published in PRD and Rapid Communications

Work supported in part by US Department of Energy contract DE-AC02-76SF00515

D. Lopes Pegna,[61] C. Lu,[61] J. Olsen,[61] A. J. S. Smith,[61] A. V. Telnov,[61] F. Anulli[a],[62] E. Baracchini[ab],[62] G. Cavoto[a],[62] R. Faccini[ab],[62] F. Ferrarotto[a],[62] F. Ferroni[ab],[62] M. Gaspero[ab],[62] P. D. Jackson[a],[62] L. Li Gioi[a],[62] M. A. Mazzoni[a],[62] S. Morganti[a],[62] G. Piredda[a],[62] F. Renga[ab],[62] C. Voena[a],[62] M. Ebert,[63] T. Hartmann,[63] H. Schröder,[63] R. Waldi,[63] T. Adye,[64] B. Franek,[64] E. O. Olaiya,[64] F. F. Wilson,[64] S. Emery,[65] L. Esteve,[65] G. Hamel de Monchenault,[65] W. Kozanecki,[65] G. Vasseur,[65] Ch. Yèche,[65] M. Zito,[65] M. T. Allen,[66] D. Aston,[66] R. Bartoldus,[66] J. F. Benitez,[66] R. Cenci,[66] J. P. Coleman,[66] M. R. Convery,[66] J. C. Dingfelder,[66] J. Dorfan,[66] G. P. Dubois-Felsmann,[66] W. Dunwoodie,[66] R. C. Field,[66] A. M. Gabareen,[66] M. T. Graham,[66] P. Grenier,[66] C. Hast,[66] W. R. Innes,[66] J. Kaminski,[66] M. H. Kelsey,[66] H. Kim,[66] P. Kim,[66] M. L. Kocian,[66] D. W. G. S. Leith,[66] S. Li,[66] B. Lindquist,[66] S. Luitz,[66] V. Luth,[66] H. L. Lynch,[66] D. B. MacFarlane,[66] H. Marsiske,[66] R. Messner,[66, *] D. R. Muller,[66] H. Neal,[66] S. Nelson,[66] C. P. O'Grady,[66] I. Ofte,[66] M. Perl,[66] B. N. Ratcliff,[66] A. Roodman,[66] A. A. Salnikov,[66] R. H. Schindler,[66] J. Schwiening,[66] A. Snyder,[66] D. Su,[66] M. K. Sullivan,[66] K. Suzuki,[66] S. K. Swain,[66] J. M. Thompson,[66] J. Va'vra,[66] A. P. Wagner,[66] M. Weaver,[66] C. A. West,[66] W. J. Wisniewski,[66] M. Wittgen,[66] D. H. Wright,[66] H. W. Wulsin,[66] A. K. Yarritu,[66] K. Yi,[66] C. C. Young,[66] V. Ziegler,[66] X. R. Chen,[67] H. Liu,[67] W. Park,[67] M. V. Purohit,[67] R. M. White,[67] J. R. Wilson,[67] P. R. Burchat,[68] A. J. Edwards,[68] T. S. Miyashita,[68] S. Ahmed,[69] M. S. Alam,[69] J. A. Ernst,[69] B. Pan,[69] M. A. Saeed,[69] S. B. Zain,[69] S. M. Spanier,[70] B. J. Wogsland,[70] R. Eckmann,[71] J. L. Ritchie,[71] A. M. Ruland,[71] C. J. Schilling,[71] R. F. Schwitters,[71] B. C. Wray,[71] B. W. Drummond,[72] J. M. Izen,[72] X. C. Lou,[72] F. Bianchi[ab],[73] D. Gamba[ab],[73] M. Pelliccioni[ab],[73] M. Bomben[ab],[74] L. Bosisio[ab],[74] C. Cartaro[ab],[74] G. Della Ricca[ab],[74] L. Lanceri[ab],[74] L. Vitale[ab],[74] V. Azzolini,[75] N. Lopez-March,[75] F. Martinez-Vidal,[75] D. A. Milanes,[75] A. Oyanguren,[75] J. Albert,[76] Sw. Banerjee,[76] B. Bhuyan,[76] H. H. F. Choi,[76] K. Hamano,[76] G. J. King,[76] R. Kowalewski,[76] M. J. Lewczuk,[76] I. M. Nugent,[76] J. M. Roney,[76] R. J. Sobie,[76] T. J. Gershon,[77] P. F. Harrison,[77] J. Ilic,[77] T. E. Latham,[77] G. B. Mohanty,[77] E. M. T. Puccio,[77] H. R. Band,[78] X. Chen,[78] S. Dasu,[78] K. T. Flood,[78] Y. Pan,[78] R. Prepost,[78] C. O. Vuosalo,[78] and S. L. Wu[78]

(The BABAR Collaboration)

[1]*Laboratoire d'Annecy-le-Vieux de Physique des Particules (LAPP), Université de Savoie, CNRS/IN2P3, F-74941 Annecy-Le-Vieux, France*
[2]*Universitat de Barcelona, Facultat de Fisica, Departament ECM, E-08028 Barcelona, Spain*
[3]*INFN Sezione di Bari[a]; Dipartimento di Fisica, Università di Bari[b], I-70126 Bari, Italy*
[4]*University of Bergen, Institute of Physics, N-5007 Bergen, Norway*
[5]*Lawrence Berkeley National Laboratory and University of California, Berkeley, California 94720, USA*
[6]*University of Birmingham, Birmingham, B15 2TT, United Kingdom*
[7]*Ruhr Universität Bochum, Institut für Experimentalphysik 1, D-44780 Bochum, Germany*
[8]*University of British Columbia, Vancouver, British Columbia, Canada V6T 1Z1*
[9]*Brunel University, Uxbridge, Middlesex UB8 3PH, United Kingdom*
[10]*Budker Institute of Nuclear Physics, Novosibirsk 630090, Russia*
[11]*University of California at Irvine, Irvine, California 92697, USA*
[12]*University of California at Los Angeles, Los Angeles, California 90024, USA*
[13]*University of California at Riverside, Riverside, California 92521, USA*
[14]*University of California at San Diego, La Jolla, California 92093, USA*
[15]*University of California at Santa Barbara, Santa Barbara, California 93106, USA*
[16]*University of California at Santa Cruz, Institute for Particle Physics, Santa Cruz, California 95064, USA*
[17]*California Institute of Technology, Pasadena, California 91125, USA*
[18]*University of Cincinnati, Cincinnati, Ohio 45221, USA*
[19]*University of Colorado, Boulder, Colorado 80309, USA*
[20]*Colorado State University, Fort Collins, Colorado 80523, USA*
[21]*Technische Universität Dortmund, Fakultät Physik, D-44221 Dortmund, Germany*
[22]*Technische Universität Dresden, Institut für Kern- und Teilchenphysik, D-01062 Dresden, Germany*
[23]*Laboratoire Leprince-Ringuet, CNRS/IN2P3, Ecole Polytechnique, F-91128 Palaiseau, France*
[24]*University of Edinburgh, Edinburgh EH9 3JZ, United Kingdom*
[25]*INFN Sezione di Ferrara[a]; Dipartimento di Fisica, Università di Ferrara[b], I-44100 Ferrara, Italy*
[26]*INFN Laboratori Nazionali di Frascati, I-00044 Frascati, Italy*
[27]*INFN Sezione di Genova[a]; Dipartimento di Fisica, Università di Genova[b], I-16146 Genova, Italy*
[28]*Harvard University, Cambridge, Massachusetts 02138, USA*
[29]*Universität Heidelberg, Physikalisches Institut, Philosophenweg 12, D-69120 Heidelberg, Germany*
[30]*Humboldt-Universität zu Berlin, Institut für Physik, Newtonstr. 15, D-12489 Berlin, Germany*
[31]*Imperial College London, London, SW7 2AZ, United Kingdom*
[32]*University of Iowa, Iowa City, Iowa 52242, USA*
[33]*Iowa State University, Ames, Iowa 50011-3160, USA*
[34]*Johns Hopkins University, Baltimore, Maryland 21218, USA*

[35]Laboratoire de l'Accélérateur Linéaire, IN2P3/CNRS et Université Paris-Sud 11,
Centre Scientifique d'Orsay, B. P. 34, F-91898 Orsay Cedex, France
[36]Lawrence Livermore National Laboratory, Livermore, California 94550, USA
[37]University of Liverpool, Liverpool L69 7ZE, United Kingdom
[38]Queen Mary, University of London, London, E1 4NS, United Kingdom
[39]University of London, Royal Holloway and Bedford New College, Egham, Surrey TW20 0EX, United Kingdom
[40]University of Louisville, Louisville, Kentucky 40292, USA
[41]Johannes Gutenberg-Universität Mainz, Institut für Kernphysik, D-55099 Mainz, Germany
[42]University of Manchester, Manchester M13 9PL, United Kingdom
[43]University of Maryland, College Park, Maryland 20742, USA
[44]University of Massachusetts, Amherst, Massachusetts 01003, USA
[45]Massachusetts Institute of Technology, Laboratory for Nuclear Science, Cambridge, Massachusetts 02139, USA
[46]McGill University, Montréal, Québec, Canada H3A 2T8
[47]INFN Sezione di Milano[a]; Dipartimento di Fisica, Università di Milano[b], I-20133 Milano, Italy
[48]University of Mississippi, University, Mississippi 38677, USA
[49]Université de Montréal, Physique des Particules, Montréal, Québec, Canada H3C 3J7
[50]Mount Holyoke College, South Hadley, Massachusetts 01075, USA
[51]INFN Sezione di Napoli[a]; Dipartimento di Scienze Fisiche,
Università di Napoli Federico II[b], I-80126 Napoli, Italy
[52]NIKHEF, National Institute for Nuclear Physics and High Energy Physics, NL-1009 DB Amsterdam, The Netherlands
[53]University of Notre Dame, Notre Dame, Indiana 46556, USA
[54]Ohio State University, Columbus, Ohio 43210, USA
[55]University of Oregon, Eugene, Oregon 97403, USA
[56]INFN Sezione di Padova[a]; Dipartimento di Fisica, Università di Padova[b], I-35131 Padova, Italy
[57]Laboratoire de Physique Nucléaire et de Hautes Energies,
IN2P3/CNRS, Université Pierre et Marie Curie-Paris6,
Université Denis Diderot-Paris7, F-75252 Paris, France
[58]University of Pennsylvania, Philadelphia, Pennsylvania 19104, USA
[59]INFN Sezione di Perugia[a]; Dipartimento di Fisica, Università di Perugia[b], I-06100 Perugia, Italy
[60]INFN Sezione di Pisa[a]; Dipartimento di Fisica,
Università di Pisa[b]; Scuola Normale Superiore di Pisa[c], I-56127 Pisa, Italy
[61]Princeton University, Princeton, New Jersey 08544, USA
[62]INFN Sezione di Roma[a]; Dipartimento di Fisica,
Università di Roma La Sapienza[b], I-00185 Roma, Italy
[63]Universität Rostock, D-18051 Rostock, Germany
[64]Rutherford Appleton Laboratory, Chilton, Didcot, Oxon, OX11 0QX, United Kingdom
[65]CEA, Irfu, SPP, Centre de Saclay, F-91191 Gif-sur-Yvette, France
[66]SLAC National Accelerator Laboratory, Stanford, California 94309 USA
[67]University of South Carolina, Columbia, South Carolina 29208, USA
[68]Stanford University, Stanford, California 94305-4060, USA
[69]State University of New York, Albany, New York 12222, USA
[70]University of Tennessee, Knoxville, Tennessee 37996, USA
[71]University of Texas at Austin, Austin, Texas 78712, USA
[72]University of Texas at Dallas, Richardson, Texas 75083, USA
[73]INFN Sezione di Torino[a]; Dipartimento di Fisica Sperimentale, Università di Torino[b], I-10125 Torino, Italy
[74]INFN Sezione di Trieste[a]; Dipartimento di Fisica, Università di Trieste[b], I-34127 Trieste, Italy
[75]IFIC, Universitat de Valencia-CSIC, E-46071 Valencia, Spain
[76]University of Victoria, Victoria, British Columbia, Canada V8W 3P6
[77]Department of Physics, University of Warwick, Coventry CV4 7AL, United Kingdom
[78]University of Wisconsin, Madison, Wisconsin 53706, USA

(Dated: June 2, 2009)

We have performed a search for the rare leptonic decays $B^+ \to \ell^+\nu_\ell$ ($l = e, \mu$), using data collected at the $\Upsilon(4S)$ resonance by the *BABAR* detector at the PEP-II storage ring. In a sample of 468 million $B\overline{B}$ pairs we find no evidence for a signal and set an upper limit on the branching fractions $\mathcal{B}(B^+ \to \mu^+\nu_\mu) < 1.0 \times 10^{-6}$ and $\mathcal{B}(B^+ \to e^+\nu_e) < 1.9 \times 10^{-6}$ at the 90% confidence level, using a Bayesian approach.

PACS numbers: 13.20.-v, 13.25.Hw

In the standard model (SM), the purely leptonic B meson decays $B^+ \to \ell^+\nu_\ell$ [1] proceed at lowest order through the annihilation diagram shown in Fig. 1. The SM branching fraction can be calculated as [2]

$$\mathcal{B}(B^+ \to \ell^+\nu_\ell) = \frac{G_F^2 m_B m_\ell^2}{8\pi}\left(1 - \frac{m_\ell^2}{m_B^2}\right)^2 f_B^2 |V_{ub}|^2 \tau_B, \tag{1}$$

where G_F is the Fermi coupling constant, m_ℓ and m_B are respectively the lepton and B meson masses, and τ_B is the B^+ lifetime. The decay rate is sensitive to the CKM matrix element $|V_{ub}|$ [3] and the B decay constant f_B that describes the overlap of the quark wave functions within the meson.

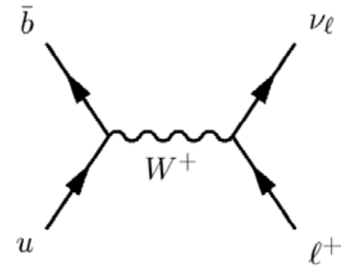

FIG. 1: Lowest order SM Feynman diagram for the purely leptonic decay $B^+ \to l^+\nu_l$.

The SM estimate of the branching fraction for $B^+ \to \tau^+\nu_\tau$ is $(1.59 \pm 0.40) \times 10^{-4}$ assuming $\tau_B = 1.638\pm0.011$ ps [4], $V_{ub} = (4.39\pm0.33)\times10^{-3}$ determined from inclusive charmless semileptonic B decays [5] and $f_B = 216\pm22$ MeV from lattice QCD calculation [6]. To a very good approximation, helicity is conserved in $B^+ \to \mu^+\nu_\mu$ and $B^+ \to e^+\nu_e$ decays, which are therefore suppressed by factors $m^2_{\mu,e}/m^2_\tau$ with respect to $B^+ \to \tau^+\nu_\tau$, leading to expected branching fractions of $\mathcal{B}(B^+ \to \mu^+\nu_\mu) = (5.6\pm0.4)\times10^{-7}$ and $\mathcal{B}(B^+ \to e^+\nu_e) = (1.3\pm0.4)\times10^{-11}$. However, reconstruction of $B^+ \to \tau^+\nu_\tau$ decays is experimentally more challenging than $B^+ \to \mu^+\nu_\mu$ or $B^+ \to e^+\nu_e$ due to the large missing momentum from multiple neutrinos in the final state.

Purely leptonic B decays are sensitive to physics beyond the SM, where additional heavy virtual particles contribute to the annihilation processes. Charged Higgs boson effects may greatly enhance or suppress the branching fraction in some two-Higgs-doublet models [7]. Similarly, there may be enhancements through mediation by leptoquarks in the Pati-Salam model of quark-lepton unification [8]. Direct tests of Yukawa interactions in and beyond the SM are possible in the study of these decays, as annihilation processes proceed through the longitudinal component of the intermediate vector boson. In particular, in a SUSY scenario at large $\tan\beta$, non-standard effects in helicity-suppressed charged current interactions are potentially observable, being strongly $\tan\beta$-dependent and leading to [7]:

$$\frac{\mathcal{B}(B^+ \to l^+\nu_l)_{\rm exp}}{\mathcal{B}(B^+ \to l^+\nu_l)_{\rm SM}} \approx (1 - \tan^2\beta \frac{m_B^2}{M_H^2})^2. \tag{2}$$

Evidence for the first purely leptonic B decays has recently been presented by both the BABAR and Belle collaborations. The latest HFAG world average of the BABAR [9] and Belle [10] results is $\mathcal{B}(B^+ \to \tau^+\nu_\tau) = (1.51 \pm 0.33) \times 10^{-4}$ [11]. The current best published upper limits on $B^+ \to \mu^+\nu_\mu$ and $B^+ \to e^+\nu_e$ are $\mathcal{B}(B^+ \to \mu^+\nu_\mu) < 1.7 \times 10^{-6}$ and $\mathcal{B}(B^+ \to e^+\nu_e) < 9.8 \times 10^{-7}$ at 90% confidence level from Belle using a data sample of 235 fb^{-1} [12].

The analysis described in herein is based on the entire dataset collected with the BABAR detector [13] at the PEP-II storage ring at the $\Upsilon(4S)$ resonance ("on-resonance"), which consists of 468 million $B\overline{B}$ pairs, corresponding to an integrated luminosity of 426 fb^{-1}. In order to study background from continuum events such as $e^+e^- \to q\bar{q}$ ($q = u, d, s, c$) and $e^+e^- \to \tau^+\tau^-$, an additional sample of about 41 fb^{-1} was collected at a center-of-mass (c.m.) energy about 40 MeV below the $\Upsilon(4S)$ resonance ("off-resonance").

In the BABAR detector, charged particle trajectories are measured with a 5-layer double-sided silicon vertex tracker and a 40-layer drift chamber, which are contained in the 1.5 T magnetic field of a superconducting solenoid. A detector of internally reflected Cherenkov radiation provides identification of charged kaons and pions. The energies and trajectories of neutral particles are measured by an electromagnetic calorimeter consisting of 6580 CsI(Tl) crystals. The flux return of the solenoid is instrumented with resistive plate chambers and, more recently, limited streamer tubes [14], in order to provide muon identification. A `GEANT4`-based [15] Monte Carlo (MC) simulation of generic $B\bar{B}$, $q\bar{q}$, $q = u, d, s, c$, and $\tau^+\tau^-$ events as well as $B^+ \to \mu^+\nu_\mu$ and $B^+ \to e^+\nu_e$ signal events is used to model the detector response and test the analysis technique.

The $B^+ \to \ell^+\nu_\ell$ decay produces a mono-energetic charged lepton in the B rest frame with a momentum $p^* \approx m_B/2$. The B mesons produced in $\Upsilon(4S)$ decays have a c.m. momentum of about 320 MeV/c, so we initially select lepton candidates with c.m. momentum 2.4 $< p_{\rm c.m.} <$ 3.2 GeV/c, to take into account the smearing due to the motion of the B. A tight particle identification requirement is applied to the candidate lepton in order to discard fake muons or electrons.

Since the neutrino produced in the signal decay is not detected, all charged tracks besides the signal lepton and all neutral energy deposits in the calorimeter are combined to reconstruct the companion (tag) B. We include all neutral calorimeter clusters with cluster energy greater than 30 MeV. Particle identification is applied to the charged tracks to identify electrons, muons, pions, kaons and protons in order to assign the most likely mass hypothesis to each $B_{\rm tag}$ daughter and thus improve the reconstruction of the $B_{\rm tag}$. Events which have additional lepton candidates are discarded. These typically arise from semileptonic $B_{\rm tag}$ or charm decays and indicate the presence of additional neutrinos, for which the inclusive $B_{\rm tag}$ reconstruction is not expected to work well.

The signal lepton's momentum in the signal B rest frame p^* is refined using the $B_{\rm tag}$ momentum direction. We assume that the signal B has a c.m. momentum of 320 MeV/c and choose its direction as opposite that of the reconstructed $B_{\rm tag}$ to boost the lepton candidate into the signal B rest frame.

Signal events are selected using the kinematic variables $\Delta E = E_B - E_{\rm beam}$, where E_B is the energy of the $B_{\rm tag}$ and $E_{\rm beam}$ is the beam energy, all in the c.m. frame. For signal events in which all decay products of the $B_{\rm tag}$ are reconstructed, we expect the ΔE distribution to peak near zero. However, we are often unable to reconstruct all $B_{\rm tag}$ decay products, which biases the ΔE distribution toward negative values. For continuum backgrounds, ΔE is shifted toward relatively large positive values since too much energy is attributed to the nominal $B_{\rm tag}$ decay, while there is a negative bias in $\tau^+\tau^-$ events due to the unreconstructed neutrinos.

We require the tag B to satisfy $-2.25 < \Delta E < 0$ GeV for $B^+ \to \mu^+\nu_\mu$ decays. For $B^+ \to e^+\nu_e$ decays, we require a linear combination of ΔE and the tag B transverse momentum p_T to satisfy $(p_T + 0.529 \cdot \Delta E)$ <0.2 and $(p_T - 0.529 \cdot \Delta E)$ <1.5. This selection rejects background events arising from two-photon process $e^+e^- \to e^+e^-\gamma^*\gamma^*$, $\gamma^*\gamma^* \to hadrons$ with one of the final electrons scattered at a large angle and detected. The coefficient of the ΔE term is extracted from the data.

Backgrounds may arise from any process producing charged tracks in the momentum range of the signal, particularly if the charged tracks are leptons. The two most significant backgrounds are B semileptonic decays involving $b \to u l \nu_l$ transitions in which the momentum of the leptons at the endpoint of the spectrum approaches that of the signal, and from continuum and $\tau^+\tau^-$ events in which a charged pion is mistakenly identified as a muon or an electron.

Continuum events tend to produce a jet-like event topology, while $B\overline{B}$ events tend to be more isotropically distributed in the c.m. frame, and are suppressed using event shape parameters. Five different spatial and kinematical variables, considered separately for $B^+ \to \mu^+\nu_\mu$ and $B^+ \to e^+\nu_e$, are combined in Fisher discriminants [16]. The most effective discriminating parameters are the ratio of the second L_2 and the zeroth L_0 monomial $L_n = \Sigma_i |\vec{p}_i| \cos(\alpha)^n$, where the sum runs over all $B_{\rm tag}$ daughters having momenta $\vec{p}_i$ and α is the angle with respect to the lepton candidate momentum, both in the c.m. frame, and the sphericity $S = \frac{3}{2}\min\frac{\Sigma_j (p_{jT})^2}{\Sigma_j (p_j)^2}$, where the T subscript denotes the momentum component transverse to the sphericity axis, which is the axis that minimizes S. S, in fact, tends to be closer to 1 for spherical events and 0 for jet-like events. In order to take into account the changes in detector performance throughout the years, in particular in muon identification, the data sample is divided into six different data taking periods, and the Fisher discriminants and selection criteria are optimized separately with the algorithm described in [17] for each period.

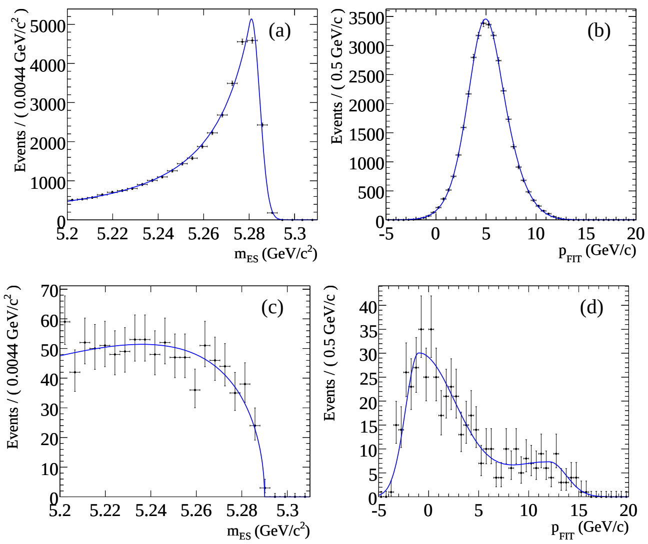

FIG. 2: Distributions of signal (a,b) and background (c,d) m_{ES} (left) and $p_{\rm FIT}$ (right) for $B^+ \to \mu^+\nu_\mu$ from MC simulation (a,b and c) and from m_{ES} sideband $5.17 < m_{ES} < 5.2$ GeV/c^2 (d).

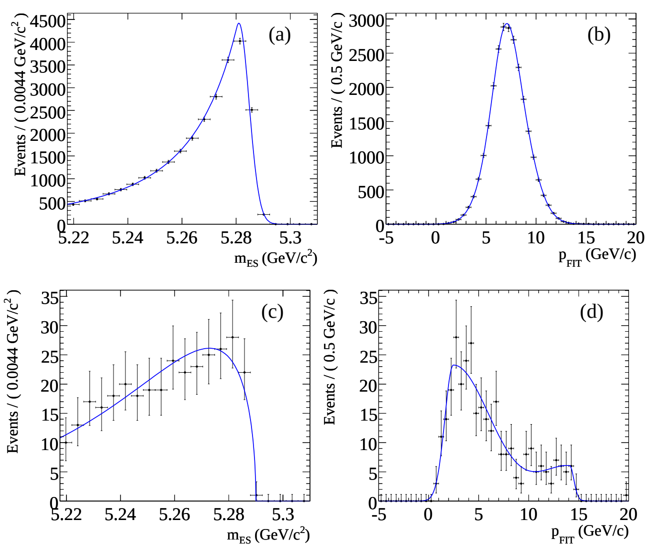

FIG. 3: Distributions of signal (a,b) and background (c,d) m_{ES} (left) and $p_{\rm FIT}$ (right) for $B^+ \to e^+\nu_e$ from MC simulation.

The two-body kinematics of the signal decay is exploited by combining the signal lepton momentum in the B rest frame p^* and $p_{\rm c.m.}$ in a second Fisher discriminant ($p_{\rm FIT}$) which discriminates against the remaining semileptonic $b\bar{b}$ and continuum background events which populate the end of the lepton spectrum in both frames. The p^* and $p_{\rm c.m.}$ coefficients in the linear combination are determined separately for $B^+ \to \mu^+\nu_\mu$ and $B^+ \to e^+\nu_e$ with [17].

We employ an extended maximum likelihood (ML) fit to extract signal and background yields using simultaneously the distributions of the Fisher output $p_{\rm FIT}$ and the energy-substituted mass $m_{\rm ES}$, defined as $\sqrt{E^2_{\rm beam} - |\vec{p}_B|^{\,2}}$, where $\vec{p}_B$ is the momentum of the reconstructed $B_{\rm tag}$ candidate in the c.m. frame.

Signal m_{ES} and $p_{\rm FIT}$ probability density functions (PDFs) are fixed in the final fit and are parameterized from simulated events, respectively, with a Crystal Ball function [18] and the sum of two Gaussians (double Gaussian) for both $B^+ \to \mu^+\nu_\mu$ and $B^+ \to e^+\nu_e$.

The background m_{ES} distribution is described by an ARGUS function whose slope is determined in the fit to the yields [19]. To parameterize the background $p_{\rm FIT}$ distributions, we studied the possibility of using the m_{ES} sideband of on-resonance data. We found the $B^+ \to \mu^+\nu_\mu$ sideband suited for this purpose, while the $B^+ \to e^+\nu_e$ sideband is not sufficiently populated. We use the region $5.17 < m_{ES} < 5.2$ GeV/c^2 to parameterize the $B^+ \to \mu^+\nu_\mu$ background $p_{\rm FIT}$ distribution, and simulated events for the background $B^+ \to e^+\nu_e$ $p_{\rm FIT}$ distribution.

Separately for $B^+ \to \mu^+\nu_\mu$ and $B^+ \to e^+\nu_e$, the sum of two Gaussians with different sigmas on the right and the left of the mean (bifurcated Gaussians) is used to parameterize the background $p_{\rm FIT}$ distribution and the relative fraction of the two bifurcated Gaussians is determined from the fit to the data. Figures 2 and 3 show background and signal m_{ES} and $p_{\rm FIT}$ distributions for $B^+ \to \mu^+\nu_\mu$ and $B^+ \to e^+\nu_e$, respectively, with the PDFs described above superimposed.

In the on-resonance data the ML fit returns 1 ± 15 signal $B^+ \to \mu^+\nu_\mu$ candidate events and 18 ± 14 signal $B^+ \to e^+\nu_e$ candidate events. Distributions of the fit data events with the final fit superimposed, as well as the signal and background PDFs, are shown in Figure 4 for $B^+ \to \mu^+\nu_\mu$ and $B^+ \to e^+\nu_e$, respectively, projected on m_{ES} and $p_{\rm FIT}$.

We next evaluate systematic uncertainties on the number of $B^\pm$ in the sample, the signal efficiency and the signal yield. The number of $B^\pm$ mesons in the on-resonance data sample is estimated to be 468×10^6 with an uncertainty of 1.1% [20], assuming equal B^+ and B^0 production at the $\Upsilon(4S)$ [21].

The uncertainty in the signal efficiency includes the lepton candidate selection (particle identification, tracking efficiency and event selection Fisher requirement) as well as the reconstruction efficiency of the tag B. The systematic uncertainty on the particle identification efficiency is evaluated using $e^+e^- \to \mu^+\mu^-\gamma$, $e^+e^- \to e^+e^-\mu^+\mu^-$ and Bhabha event control samples derived from the data, which are weighted to reproduce the kinematic distribution of the lepton signal candidate. Comparing the cumulative signal efficiency obtained with and without these weights, a total discrepancy of 1.9% for $B^+ \to \mu^+\nu_\mu$ and 2.3% for $B^+ \to e^+\nu_e$ is found and this value is taken as the particle identification systematic uncertainty. Tracking efficiency is studied employing τ decays, which must produce an odd number of final state charged tracks because of charge conservation. Thus, one can determine an absolute efficiency because the number of events with a missing track can be measured. The uncertainty associated with the tracking efficiency and the data/MC discrepancy evaluated with this method are taken in quadrature for a total tracking efficiency uncertainty of 0.4% per track.

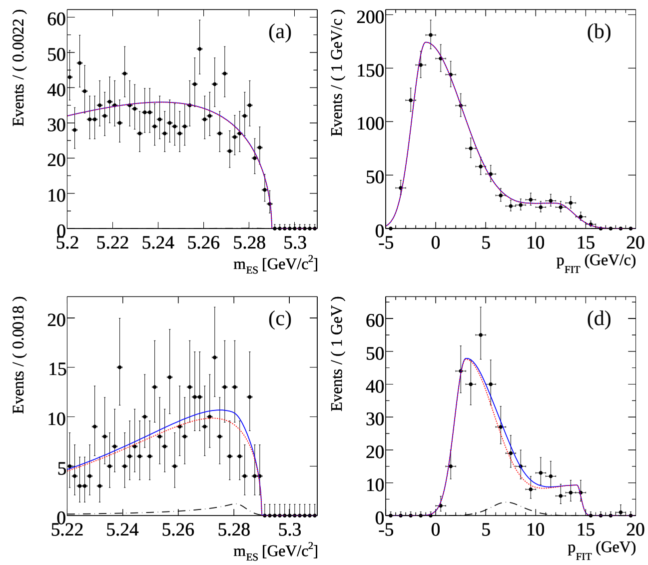

FIG. 4: Final fit to the data projected on m_{ES} (left) and $p_{\rm FIT}$ (right) distributions for $B^+ \to \mu^+\nu_\mu$ events (a,b) and $B^+ \to e^+\nu_e$ events (c,d) : the solid blue line is the total PDF, the dashed red line is the background PDF and the dashed-dotted black line is the signal PDF

In order to evaluate the systematic uncertainty associated with the requirements on the Fisher discriminants, we compare data and MC Fisher distributions in the sidebands ΔE¿0 for the $B^+ \to \mu^+\nu_\mu$ sample and $(p_T + 0.529 \cdot \Delta E)$¿ 0.2 for the $B^+ \to e^+\nu_e$ sample. We fit the data/MC ratio with a linear function, with results consistent with a unitary ratio in the whole Fishers range. We take the error on the intercept as the systematic uncertainty on the Fisher discriminants, that is 1.4 % for $B^+ \to \mu^+\nu_\mu$ and 5.3% for $B^+ \to e^+\nu_e$.

The tag B reconstruction has been studied with a control sample of $B^+ \to D^{(*)0}\pi^+$ events, where the D is reconstructed into $\bar{D}^0 \to K^+\pi^-$ and $D^0 \to K^-\pi^+$, and the D^* into $D^{*0} \to D^0\gamma$ or $D^{*0} \to D^0\pi^0$. These two-

TABLE I: Contributions to the systematic uncertainty on the signal efficiency. Total systematic represent the sum in quadrature of the table entries.

Source	$B^+ \to \mu^+\nu_\mu$	$B^+ \to e^+\nu_e$
Particle identification	1.9%	2.3 %
Tracking efficiency	0.4%	0.4 %
Tag B reconstruction	3.0%	0.4 %
Fisher selection	1.4%	5.3 %
Total	3.8%	5.8 %

body decays are topologically very similar to our signal, as the charged pion can be treated as the signal lepton and the $D^{(*)0}$ decays products ignored to simulate the missing neutrino. The tag B reconstructed in the control sample thus simulates the tag B reconstruction in the nominal data sample. We compare the efficiencies for our tag B selection cuts in the $B^+ \to D^{(*)0}\pi^+$ data and MC to quantify any data/MC disagreements that may affect the signal efficiency. We find a data/MC discrepancy on $B^+ \to D^{(*)0}\pi^+$ control sample of 3.0% for $B^+ \to \mu^+\nu_\mu$ decays and 0.4% for $B^+ \to e^+\nu_e$ decays, and assign these as the signal efficiency uncertainty arising from the tag B selection.

A summary of the systematic uncertainties in the signal efficiency is given in Table I. The final $B^+ \to \mu^+\nu_\mu$ signal efficiency is (6.1 $\pm$ 0.2)% and the $B^+ \to e^+\nu_e$ signal efficiency is (4.7 $\pm$ 0.3)%, where the errors are the sum in quadrature of statistical and systematic uncertainties.

The systematic uncertainty in the yields comes from the $p_{\rm FIT}$ and m_{ES} PDF parameters, which are kept fixed in the final fit and, in the $B^+ \to e^+\nu_e$ case, from the use of MC simulation to extract the PDF shapes. The fit parameters extracted from MC are affected by an uncertainty due to MC statistics. In order to evaluate the systematic uncertainty associated with the parameterization, the final fit has been repeated 500 times for each background and signal PDF parameter which is kept fixed in the final fit. We randomly generate the PDF parameters assuming Gaussian errors and taking into account all the correlations between them. We perform a Gaussian fit to the distribution of the number of signal events for each parameter, take the fitted sigma as the systematic uncertainty and sum in quadrature. The total systematic uncertainty on the signal yield from all signal and background PDF parameters is 8 events for $B^+ \to \mu^+\nu_\mu$ and 10 events for $B^+ \to e^+\nu_e$.

For the $B^+ \to e^+\nu_e$ sample, an additional systematic uncertainty coming from possible discrepancies in the shape of the $p_{\rm FIT}$ background distribution in data and simulated events must be accounted for. The data/MC ratio of the $p_{\rm FIT}$ distribution in the m_{ES} sideband 5.16 $< m_{ES} <$ 5.22 GeV/c^2 is fit with a linear function. The background $p_{\rm FIT}$ distribution shape is varied according to the fitted linear function and its associated statistical uncertainties; the total systematic contribution from this procedure is 4 events.

To evaluate the branching fraction we use the following expression:

$$\mathcal{B}(B \to l^+\nu)_{UL} = \frac{N_{sig}}{N_{B^\pm} \cdot \varepsilon}, \tag{3}$$

where N_{sig} represents the observed signal yield, $N_{B^\pm}$ the number of B^+B^- in the sample (where equal production of B^+B^- and $B^0\bar{B}^0$ is assumed) and ε is the signal efficiency.

As we did not find evidence for signal events, we employ a Bayesian approach to set upper limits on the branching fractions. Flat prior in the branching fractions are assumed for positive values of the branching fractions and Gaussian likelihoods are adopted for the observed signal yield, related to $\mathcal{B}$ by Eq.(3). The Gaussian widths are fixed to the sum in quadrature of the statistical and systematic yield errors. The effect of systematic uncertainties associated with the efficiencies, modeled by Gaussian PDFs, is taken into account as well. We extract the following 90 % confidence level upper limits on the branching fractions:

$$\mathcal{B}(B^+ \to \mu^+\nu_\mu) \; < \; 1.0 \times 10^{-6} \tag{4}$$

$$\mathcal{B}(B^+ \to e^+\nu_e) \; < \; 1.9 \times 10^{-6}. \tag{5}$$

The 95% upper limits are $\mathcal{B}(B^+ \to \mu^+\nu_\mu) < 1.3 \times 10^{-6}$ and $\mathcal{B}(B^+ \to e^+\nu_e) < 2.2 \times 10^{-6}$. This result improves the previous best published limit for $B^+ \to \mu^+\nu_\mu$ branching fraction by nearly a factor two, to a value twice the SM prediction. The $B^+ \to e^+\nu_e$ result is consistent with previous measurements. It should be noted that the results in [12] are obtained using a different statistical approach to interpret the observed number of signal events. The results show no deviation from the SM expectations.

We are grateful for the excellent luminosity and machine conditions provided by our PEP-II colleagues, and for the substantial dedicated effort from the computing organizations that support BABAR. The collaborating institutions wish to thank SLAC for its support and kind hospitality. This work is supported by DOE and NSF (USA), NSERC (Canada), CEA and CNRS-IN2P3 (France), BMBF and DFG (Germany), INFN (Italy), FOM (The Netherlands), NFR (Norway), MES (Russia), MEC (Spain), and STFC (United Kingdom). Individuals have received support from the Marie Curie EIF (European Union) and the A. P. Sloan Foundation.

* Deceased

† Now at Temple University, Philadelphia, Pennsylvania 19122, USA

‡ Now at Tel Aviv University, Tel Aviv, 69978, Israel
§ Also with Università di Perugia, Dipartimento di Fisica, Perugia, Italy
¶ Also with Università di Roma La Sapienza, I-00185 Roma, Italy
** Now at University of South Alabama, Mobile, Alabama 36688, USA
†† Also with Laboratoire de Physique Nucléaire et de Hautes Energies, IN2P3/CNRS, Université Pierre et Marie Curie-Paris6, Université Denis Diderot-Paris7, F-75252 Paris, France
‡‡ Also with Università di Sassari, Sassari, Italy

[1] Charge conjugation is implied throughout the paper.
[2] D. Silverman and H. Yao, Phys. Rev. D **38**, 214 (1988).
[3] N. Cabibbo, Phys. Rev. Lett. **10**, 531 (1963); M. Kobayashi and T. Maskawa, Prog. Theor. Phys. **49**, 652 (1973).
[4] C. Amsler *et al.*, Physics Letters B **667**, 1 (2008).
[5] E. Barberio *et al.* [Heavy Flavor Averaging Group (HFAG)], arXiv:hep-ex/0603003.
[6] A. Gray *et al.* [HPQCD Collaboration], Phys. Rev. Lett. **95**, 212001 (2005).
[7] W. S. Hou, Phys. Rev. D **48**, 2342 (1993).
[8] G. Valencia and S. Willenbrock, Phys. Rev. D **50**, 6843 (1994).
[9] B. Aubert *et al.* [*BABAR* Collaboration], Phys. Rev. D **77**, 011107 (2008).
[10] I. Adachi *et al.* [Belle Collaboration], arXiv:0809.3834 [hep-ex].
[11] Heavy Flavor Averaging Group (HFAG), `http://www.slac.stanford.edu/xorg/hfag/index.html`.
[12] N. Satoyama *et al.* [Belle Collaboration], Phys. Lett. B **647**, 67 (2007).
[13] B. Aubert *et al.* [*BABAR* Collaboration], Nucl. Instrum. Methods A **479**, 1 (2002).
[14] G. Benelli, K. Honscheid, E. A. Lewis, J. J. Regensburger and D. S. Smith, IEEE Nucl. Sci. Symp. Conf. Rec. **2**, 1145 (2006).
[15] S. Agostinelli *et al.* [GEANT4 Collaboration], Nucl. Instrum. Methods A **506**, 250 (2003).
[16] R. A. Fisher, Ann. Eugenics **7**, 179 (1936); G. Cowan, *Statistical Data Analysis*, (Oxford University Press, 1998), p. 51.
[17] I. Narsky, arXiv:physics/0507143.
[18] J. Gaiser *et al.*, Phys. Rev. D **34**, 711 (1986).
[19] H. Albrecht *et al.*, [ARGUS Collaboration] Phys. Lett. B **241**, 278 (1990).
[20] B. Aubert *et al.* [BABAR Collaboration], Phys. Rev. D **67**, (2003) 032002.
[21] B. Aubert *et al.* [*BABAR* Collaboration], Phys. Rev. Lett. **95**, 042001 (2005).